

CNN-Based Algorithm for Drusen Identification

Paolo Checco and Fernando Corinto

Dept. of Electronics

Politecnico di Torino

Turin, Italy

Email: {paolo.checco, fernando.corinto}@polito.it

Abstract—Drusen characterize the age-related macular degeneration. Automatic procedures for their identification have been recently developed. In this paper a cellular neural network based algorithm for drusen identification in fundus photograph is proposed. The algorithm is composed by different image processing steps: noise reduction, histogram normalization and a novel procedure of adaptive segmentation. The algorithm has been validate by using images provided from an ophthalmic medical center.

I. INTRODUCTION

Age-related macular degeneration (AMD) is the leading cause of visual loss in people over the age of 65 years in the Western world and it is characterized by subretinal deposits known as *drusen* [1]. It follows that the identification and measurement of drusen is fundamental in studies of this disease. Usually, methods for drusen identification are laborious and subjective since they are based on standard image processing operations, manually implemented using well-known image processing software tools [2]. Recently, interactive semi-automated procedures have been introduced in literature ([3], [4]), but also these methods are still based on standard image processing operations. All these methodologies perform essentially a segmentation of the medical images in order to highlight the drusen.

Medical image analysis has recently been dominated by PDE (Partial Differential Equation) methods (*e.g.* noise removing, segmentation, etc.) PDE-based algorithms present several formal and practical advantages ([5], [6].) In particular, these techniques are very suitable for medical image segmentation since they can handle any of the cavities and concavities by preserving the main features of the images. Furthermore, several complex computational problems, in particular in image processing tasks, have been successfully tackled by a new paradigm of neural networks, named Cellular Neural Networks (CNNs) [7].

In this work, we propose a CNN-based algorithm which aims to enhance drusen in monochromatic medical images. The algorithm has several steps that admit of a PDE mathematical description. It is worth observing that the algorithm can be implemented by a sequence of CNN templates performing the image processing steps. Furthermore, a VLSI implementation allows to design a complete system, embedded in ophthalmology equipments.

The manuscript is organized as follows: in Sec. II some preliminaries are given, whereas the proposed algorithm is

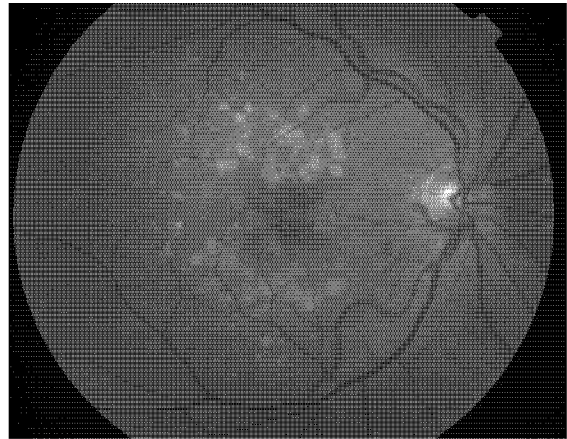


Fig. 1. High-quality monochromatic *red-free* fundus photograph in which the drusen (yellowish-white marks) are well visible.

described in Sec. III. An example showing the features of the proposed method is given in Sec. IV. In Sec. V conclusions and future possible developments are reported.

II. PRELIMINARIES

Drusen identification is performed by analyzing *color fundus photographs*, in which the drusen appear as yellowish-white marks [1]. Drusen are often better discerned on monochromatic *red-free* images when compared with color fundus photographs [2] (see Fig. 1 for an example.) It follows that the first step consist in the deletion of the red channel in RGB (Red Green Blue) color space, obtaining the *red-free* image, which is turned into a black and white one: monochromatic *red-free* image.

Once a monochromatic image is extracted, it may still exhibit random noise as well as uneven illumination and lens edge artifacts. Medical diagnosis may be more accurate and easier if images are elaborated in such a way that the important structures are highlighted through noise reduction and image segmentation, *i.e.* identification of regions with uniform gray level. We consider noise reduction as a preprocessing step useful to facilitate the drusen identification without blurring the main features of the image (drusen edges, retinal vascular trees, etc.) Furthermore, this step, acting as a nonlinear filter, is also useful to make ready the image for the segmentation and post-processing processes. These operations allow us to obtain an output image on which the drusen can be more easily detected.

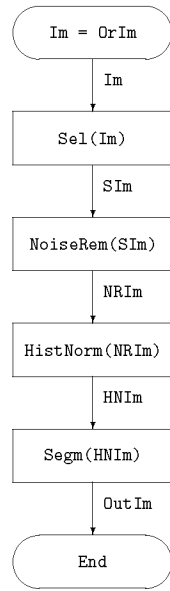


Fig. 2. Flowchart of the algorithm for drusen extraction.

In the next Section we present and describe each step of the proposed algorithm.

III. ALGORITHM

The flowchart of the proposed algorithm is reported in Fig. 2, where only the main steps are shown and the original image is called *OrIm*. We can observe that there are 4 main parts:

- *Sel(Im)*: Selection;
- *NoiseRem(SIm)*: Noise removing;
- *HistNorm(NRIm)*: Histogram normalization;
- *Segm(HNIm)*: Segmentation.

All these steps are described in the following Subsections.

A. Selection

The first step is the selection of a region of interest in the photograph under examination. This because the user (a physician) is usually interested only in some restricted regions of the fundus photograph. This step permits also to reduce the processing time. The operation is performed by the user and is applied to the monochromatic *red-free* image, obtained from the color fundus photograph (see Section II), defined as *OrIm* in the algorithm reported in Fig. 2. The output of this operation is a sub-image called *SIm*.

B. Noise Removing

The second operation consists in removing the noise. This is usually the first step in almost all image processing algorithms. The step corresponds mainly to a nonlinear filter and it can be mathematically described by a PDE. It has been shown that nonlinear isotropic filters (in particular the Perona-Malik filter [5]) are able to overcome the limitations of linear filters and are based on the idea of adapting the diffusivity to the gradient evaluated on the evolving image.

It is well known that the PDE describing the Perona-Malik nonlinear filter can be written as [5]:

$$\frac{\partial u}{\partial t} = \text{div} [g(\|\nabla u\|^2) \nabla u] \quad (1)$$

where the original image $u(0, x, y) = u_0(x, y)$ is used as initial condition, ∇u and $\|\nabla u\|$ denote the image gradient and its magnitude respectively, and $g(\cdot)$ represents the diffusivity function. The following diffusivity functions were proposed by Perona and Malik [5]:

$$g(\|\nabla u\|^2) = e^{-\left(\frac{\|\nabla u\|}{k}\right)^2} \quad (2)$$

$$g(\|\nabla u\|^2) = \left[1 + \left(\frac{\|\nabla u\|}{k}\right)^2\right]^{-1} \quad (3)$$

where k is a scalar parameter.

Finite difference approximations of Equation (1), investigated in several papers ([8]–[10]), can be exploited to obtain PDE-based CNN models that can exhibit a qualitative different dynamical behavior if the diffusivity functions are not zero only on a finite domain [6]. In particular, assuming that the continuous space domain is composed by $N \times M$ points arranged on a regular grid and denoting the position of a point with two indexes (i, j) , such that u_{ij} represents the pixel value obtained by sampling the image $u(t, x, y)$ at the point (x_i, y_j) , the following CNN equation can be easily obtained ($1 \leq i \leq N$ and $1 \leq j \leq M$):

$$\frac{d u_{ij}(t)}{dt} = \sum_{(k,l) \in N_{ij}} \Gamma_{kl} (u_{kl} - u_{ij}) \quad (4)$$

where $N_{ij} = \{(i-1, j), (i+1, j), (i, j-1), (i, j+1)\}$ and Γ_{kl} is a piecewise linear approximation of the diffusivity function (2) or (3) on a finite domain (see [6] for more details.)

The output of this process is an image in which the noise is removed almost everywhere. This output image has the same dimension of *SIm* and is named as *NRIm*.

C. Histogram Normalization

The histogram normalization redistributes the pixel intensities to equalize their distribution across the intensity range. It may be viewed as an *automatically adjusting contrast filter*. It reassigns the brightness values of pixels based on the image histogram. Individual pixels retain their brightness order (that is, they remain brighter or darker than other pixels) but the values are shifted, so that an equal number of pixels have each possible brightness value. This step is important because permits to generate images for the following steps with similar characteristics, even if the original images are different. In fact, as it has been remarked in Section II, the images are of different quality and are impaired by high level of noise as well as uneven illumination and lens edge artifacts. Thanks to this step, whose output image is called *HNIm*, the subsequent operation (see Section III-D) can be performed under the hypothesis of using a standard image.

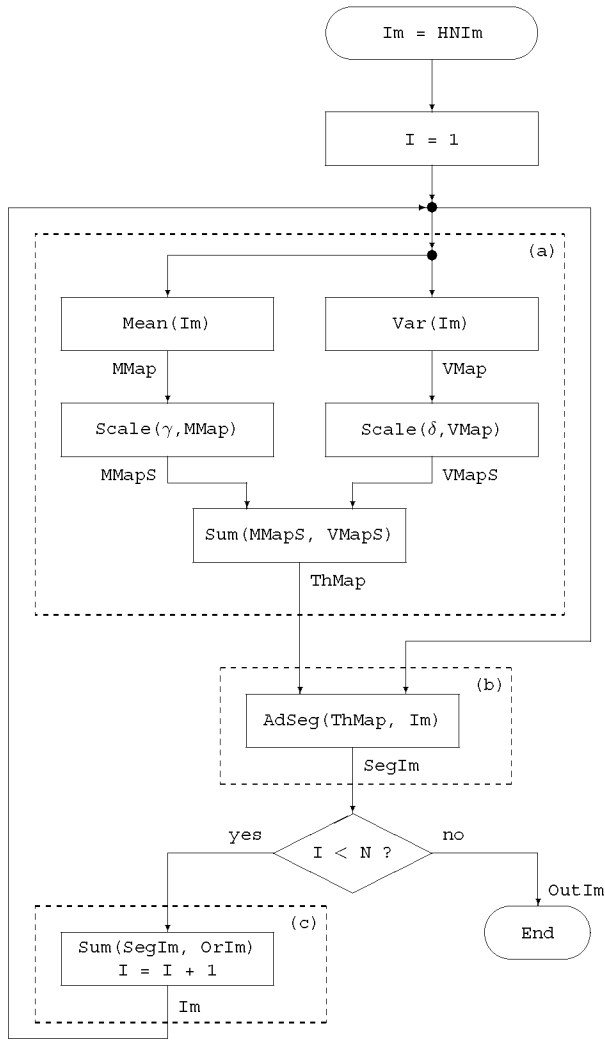


Fig. 3. Flowchart of the procedure named segmentation which receives HNIm as input and produces after N iterations the output of the algorithm.

D. Segmentation

The segmentation is the main step of the proposed algorithm since it generates an output image which contains just the useful information about the drusen. This operation executes an adaptive segmentation using a threshold map and it is an improvement of the algorithm presented in [8]. The details of this operation are reported in the flowchart shown in Fig. 3. We can identify three main parts in the algorithm:

- Estimation of a threshold map;
- Adaptive segmentation based on the threshold map;
- Generation of a new image by a sum operation.

The *estimation of a threshold map* (part (a) of the procedure shown in Fig. 3) is computed by summing two scaled maps. The first one is the image MMapS obtained by: 1) estimating the local mean value (operation Mean), calculated in the local neighborhood; 2) scaling by γ (operation Scale(γ , MMap)) the resulting image MMap. The other scaled map, denoted with VMapS, is obtained by: 1) estimating the local variance (operation Var), calculated in the local neighborhood; 2) scaling by

δ (operation Scale(δ , VMap)) the resulting image VMap. It follows that the threshold map ThMap is a linear combination of the first and the second order local statistics and defines a space-variant threshold level.

The following step is the *adaptive segmentation* (part (b) of the procedure shown in Fig. 3) that performs the segmentation operation of the image Im by using a local threshold defined by ThMap. The output of this operation is usually a binary image obtained by comparing the image Im to the threshold map ThMap. This operation is modified in our algorithm because the adaptive segmentation AdSeg(ThMap, Im) is stopped after a short time Δt , with respect to the time constant of the CNN, without converging to the binary output. The algorithm iterates the estimation of the threshold map and the adaptive segmentation. By considering these two operations for a time Δt tending to zero, the procedure is equivalent to apply an adaptive segmentation operation with a threshold map evaluated continuously.

In order to reduce the number of iterations N, it has been introduced a further step, that is the *sum operation* (part (c) of the procedure shown in Fig. 3). This allows us to reduce also the elaboration time. In fact, the adaptive segmentation operation makes the drusen lighter whereas the other parts of the image tend to become darker. It follows that adding the segmented image to the original one the information (the drusen) is kept and it is increased the convergence of the background to the black color. The value of N is chosen so that the output image is a binary one, i.e. each pixel is black or white.

IV. EXAMPLE

In this Section an example (implemented by using the MATCNN software tool [11]) is presented and only the Figures provided by the main steps of the algorithm are shown.

The input image OrIm is obtained by adding a Gaussian white noise of zero mean value and variance equal to 10^{-2} to the monochromatic *red-free* photograph reported in Fig. 1.

The first step is the *selection*, that permits to elaborate only the useful part of the image. The output of this operation is shown in Fig. 4(a). The following step is the *noise removing*, that produces the image presented in Fig. 4(b). This operation, in addition to remove the noise, performs a smoothing process useful for the following procedures. The third step is the *histogram normalization*, whose output is the image shown in Fig. 4(c). Finally, the last step is the *segmentation*. Three output images, corresponding to different iterations, are shown (Figures 4(d)-4(f)). In particular, Fig. 4(d), Fig. 4(e), and Fig. 4(f) are the outputs of the first, second, and fifth iteration, respectively. The last picture is also the output of the proposed algorithm and provides a segmented image. We remark that the output image is obtained by using only 5 iterations. Furthermore, it is worth observing that without the procedure (c) of Fig. 3 experimental results show that about 200 iterations are necessary to get a similar result.

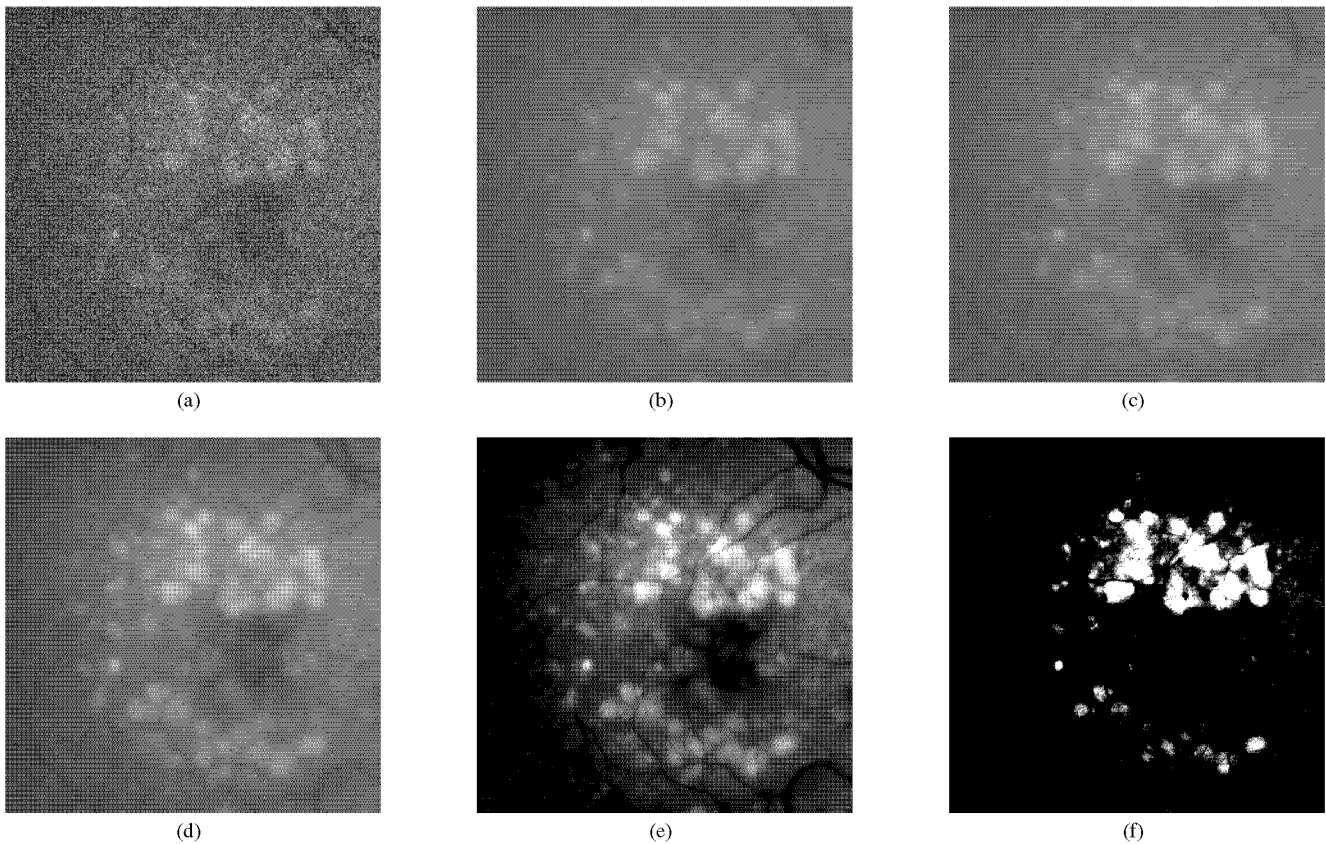


Fig. 4. Images obtained by the main steps of the algorithm shown in Fig. 2: (a) output image of the selection step; (b) image after the noise removing process; (c) image after the process of histogram normalization; (d), (e), and (f): output images of the segmentation procedure shown in Fig. 3 at the first, second, and fifth iteration, respectively.

V. CONCLUSION

Drusen characterize the AMD, which is the leading cause of visual loss in the Western world. It follows that automatic procedures for their identification are important. In this paper a CNN-based algorithm for drusen identification in fundus photographs has been proposed (Sec. III). The algorithm (Fig. 2) has the following main steps: noise reduction, histogram normalization and a novel procedure of adaptive segmentation (Fig. 3). The algorithm has been applied to images provided by an ophthalmic institute and an example is reported in Section IV. The experimental results show that the proposed algorithm may provide an accurate identification of the drusen. The comparison of the proposed method with the others above mentioned and its validation is the coming work.

VI. ACKNOWLEDGEMENTS

The authors would like to thank Dr. F. Ricci, University of Rome *Tor Vergata*, for the stimulating discussions. This work was supported by Ministero dell'Istruzione, dell'Università e della Ricerca under PRIN Project no. 2004092944_004.

REFERENCES

- [1] The age-related eye disease study research group, "The age-related eye disease study system for classifying age-related macular degeneration from stereoscopic color fundus photographs: The age-related eye disease study report number 6," *American Journal of Ophthalmology*, vol. 132, no. 5, pp. 668 – 681, Nov. 2001.
- [2] D. S. Shin, N. B. Javornik, and J. W. Berger, "Computer-assisted, interactive fundus image processing for macular drusen quantitation," *Ophthalmology*, vol. 106, no. 6, pp. 1119 – 1125, June 1999.
- [3] R. T. Smith, T. Nagasaki, J. R. Sparrow, I. Barbazetto, C. C. Klaver, and J. K. Chan, "A method of drusen measurement based on the geometry of fundus reflectance," *BioMedical Engineering OnLine*, vol. 2, no. 10, pp. 1 – 13, Apr. 2003.
- [4] R. T. Smith, J. K. Chan, T. Nagasaki, J. R. Sparrow, and I. Barbazetto, "A method of drusen measurement based on reconstruction of fundus background reflectance," *British Journal of Ophthalmology*, vol. 89, no. 1, pp. 87 – 91, Jan. 2005.
- [5] P. Perona and J. Malik, "Scale space and edge detection, using anisotropic diffusion," *IEEE Trans. Pattern Anal. Machine Intell.*, vol. 12, no. 7, pp. 629 – 639, July 1990.
- [6] F. Corinto, M. Biey, and M. Gilli, "Nonlinear coupled cnn models for multiscale image analysis," *Int. J. Circ. Theor. Appl.*, vol. 34, no. 1, pp. 77 – 88, Jan.-Feb. 2006.
- [7] L. O. Chua and L. Yang, "Cellular neural networks: Theory," *IEEE Trans. Circuits Syst.*, vol. 35, no. 10, pp. 1257 – 1272, Oct. 1988.
- [8] C. Rekeczky, "CNN architectures for constrained diffusion based locally adaptive image processing," *Int. J. Circ. Theor. Appl.*, vol. 30, no. 2 - 3, pp. 313 – 348, Mar.-June 2002.
- [9] J. Weickert, *A Review of Nonlinear Diffusion Filtering*, ser. Lecture Notes in Computer Science. Berlin: Springer, 1997, vol. 1252.
- [10] J. Weickert and B. Benhamouda, "Nonlinear diffusion scale-spaces: From the continuous to the discrete setting," in *Proc. ICAOS96: Images, Wavelets and PDEs*. New York: Springer, 1996, pp. 111–118.
- [11] C. Rekeczky, "MATCNN - analogic simulation toolbox for matlab," Analogical and Neural Computing Systems Laboratory, Computer and Automation Institute of the Hungarian Academy of Sciences, Tech. Rep. DNS-11-1997, Sept. 1997.